
Threshold fluctuations on temporally modulated backgrounds: A possible physiological explanation based upon a recent computational model

D.C. HOOD AND N. GRAHAM

Department of Psychology, Columbia University, New York

(RECEIVED November 25, 1997; ACCEPTED April 2, 1998)

Abstract

When a temporally fluctuating background is rapidly modulated (e.g. 30 Hz), the threshold variation of a superimposed flash (the probe) is approximately sinusoidal and in phase with the stimulus. But, with low rates of sinusoidal modulation (e.g. 1 Hz), the threshold variation is distinctly nonsinusoidal in shape. The bases of these aspects of the data, as well as an unmodulated, dc, threshold elevation, are poorly understood. Here 30-Hz and 1-Hz conditions are simulated using a new model of light adaptation (Wilson, 1997). By assuming that the OFF pathway is twice as sensitive as the ON pathway, the model correctly captured the key aspects of both conditions. The results suggest that the 1-Hz data are mediated by a mixture of ON and OFF pathways while the 30-Hz data are largely mediated by the OFF pathway. The probe thresholds on the 30-Hz background appear approximately sinusoidal and approximately in phase with the background stimulus. A number of factors contribute to this deceptively simple observation.

Keywords: Light adaptation, Computational model, Flicker, Incremental threshold

Introduction

Various retinal and cortical mechanisms allow the human visual system to adjust to a wide range of ambient light levels. The processes involved in this adjustment, or adaptation, to ambient lights have been extensively studied both physiologically and psychophysically. [See reviews by Hood & Finkelstein (1986) and Shapley & Enroth-Cugell (1984)]. Because of the fundamental role played by light adaptation in other visual functions, various attempts have been made to model the processes involved. A viable model would not merely help in our understanding of light adaptation itself but would provide a possible lower level module for models of higher level processing. Attempts to model adaptation, however, have failed to provide an adequate description of a broad range of behavioral data (see reviews in Graham & Hood, 1992*b*; Hood et al., 1997; Hood, 1998; Makous, 1997). Here we examine the ability of a recently proposed model (Wilson, 1997) to predict the data from a paradigm (the probed-sinewave) that has proven particularly difficult for models of light adaptation (Hood et al., 1997).

The probed-sinewave paradigm

Studies of light adaptation have, in general, employed either aperiodic (e.g. brief flashes) or periodic (usually sinusoidal) stimuli. Graham and Hood (1992*b*) argued that models originally developed to predict the results from one set of stimuli failed to predict results from the other but that the models from the two traditions could be merged to predict phenomena from both. Subsequently, merged models were developed that had some success in predicting data from a range of periodic and aperiodic paradigms (Graham & Hood, 1992*b*; von Wiegand et al., 1995). More recently, Hood et al. (1997) showed that these merged models could *not* predict the data from a paradigm (“the probed-sinewave”) that combined both aperiodic and periodic stimuli.

In this paradigm, the threshold for a brief flash (the probe) is measured at various phases of a larger background that is sinusoidally varied in time (Fig. 2A). This paradigm offers a way to describe the temporal properties of the adaptation process. To our knowledge, the first study to employ a similar paradigm was Boynton et al. (1961). They measured the threshold for a 3-ms, 1-deg probe presented upon a 2-deg background that was squarewave modulated. (Given that the visual system does not pass high frequencies very well, the results should be essentially identical for a sinusoidally modulated background.) Fig. 1 (from Boynton et al., 1961) shows the variation in probe threshold on the 30-Hz back-

All correspondence and reprint requests to: D. Hood, Department of Psychology, 406 Schermerhorn Hall, 1190 Amsterdam Avenue, Room 406, Columbia University, New York, NY 10027-7004, USA.

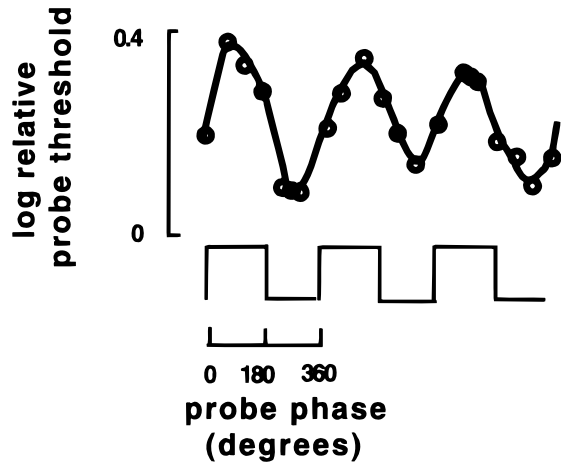


Fig. 1. Increment thresholds for a 3-ms, 1-deg probe presented upon a 2-deg background that was squarewave modulated at 30 Hz. (Modified from Fig. 2 in Boynton et al., 1961).

ground. (In Fig. 1, the lower trace shows the time course of the background.) One of the surprising findings of the Boynton et al. study was that variations in threshold tracked the 30-Hz flickering background. In particular, the variation in probe threshold was roughly sinusoidal in shape and roughly in phase with the background. There appeared to be a very fast adjustment of sensitivity. Subsequent work employing sinusoidal modulated backgrounds confirmed the Boynton et al. finding (Wu et al., 1997). On the other hand, the threshold variations with low rates of modulation are not as simply described (e.g. Shickman, 1970; Maruyama & Takahashi, 1977; Hood et al., 1997; see also abstracts by Powers & Robson, 1987; Chase et al., 1993; Bone & Chen, 1995; Sun et al., 1995). Although these studies differ in detail, a general pattern emerges. Fig. 2B from Hood et al. (1997) shows typical results from two subjects for a relatively low rate (1 Hz) of modulation. Instead of a smooth sinusoidal variation in threshold in phase with

the background modulations, the threshold variation is distinctly nonsinusoidal in shape. In the case of the data in Fig. 2B, the minimum (at about 270 deg) and maximum (at about 0 deg) are 270 deg apart, rather than 180 deg as expected of a sinewave. Further, there is a hint of an inflection near 135 deg. Some studies report a secondary peak in this region between the maximum and minimum and this peak can be quite large for the intermediate frequencies (e.g. see the 10-Hz condition in both Shickman, 1970 and Maruyama & Takahashi, 1977).

Here we compare predictions derived from Wilson's model to the 30-Hz data in Fig. 1 and the 1-Hz data in Fig. 2. For now, we avoid the intermediate background frequencies where there is a poorer agreement among existing studies (cf. Hood et al., 1997; Shickman, 1970; Maruyama & Takahashi, 1977) than there is for the low- and high-frequency conditions (cf. Boynton et al., 1961; Shickman, 1970; Maruyama & Takahashi, 1977; Wu et al., 1997). We show below that with appropriate assumptions the model proposed by Wilson provides an adequate description of the data in Figs. 1 and 2.

Wilson's model

The model proposed by Wilson (1997) is an ambitious attempt to predict a variety of results from monkey retinal physiological and human psychophysical experiments. The model will be considered in more detail in the Methods and Discussion. There are two basic reasons for considering this model. First, it successfully predicts a variety of psychophysical data including the paradigms identified by Graham and Hood (1992b) as representing basic phenomena from the two traditions (aperiodic and periodic). Second, the model differs from the models Hood et al. (1997) showed failed to adequately predict the probed-sinewave data. Although some of the basic mechanisms controlling sensitivity in the model can be found in one or more of the merged models previously considered (Graham & Hood, 1992b; Hood et al., 1997), the particular form (e.g. the heavy use of feedback) and the order and character of these mechanisms differ. Further, the model specifically includes ON and OFF pathways. In fact, there are four classes of ganglion cell in the

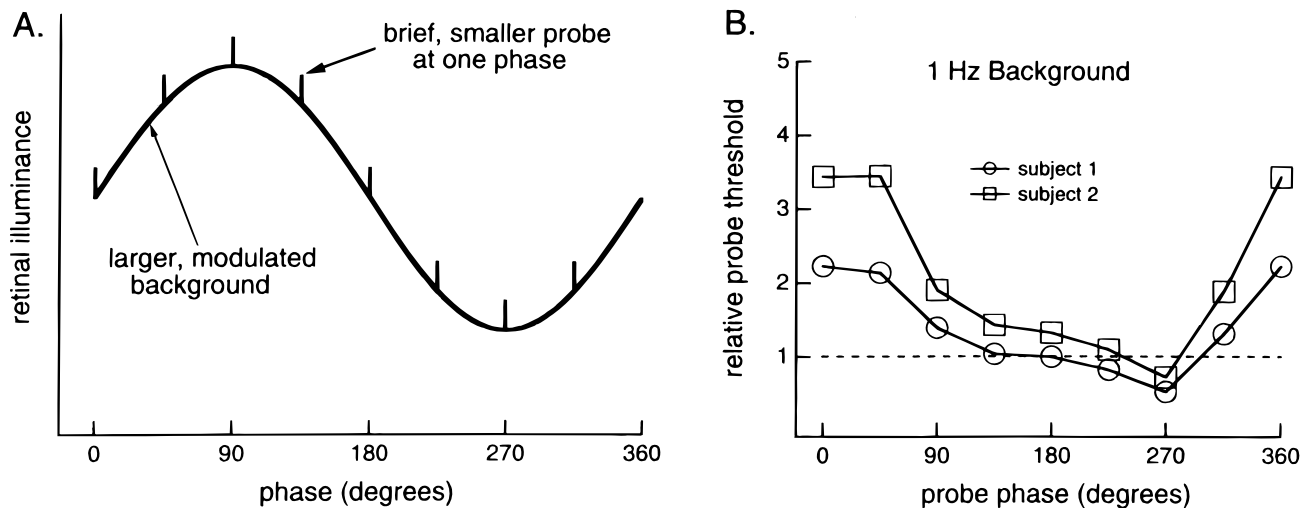


Fig. 2. A: Probed-sinewave paradigm. A brief, probe light is presented at one of a number of phases of the temporally modulated background. B: Increment thresholds for a 10-ms, 1-deg probe presented upon an 18-deg background that was sinusoidally modulated at 1 Hz (Modified from Figs. 1 and 3 in Hood et al., 1997).

model; there are ON and OFF types of both the M- and P-ganglion cells. As we will be generating predictions to relatively large, achromatic stimuli, we will use only the M-pathways. The models previously tested with probe-sinewave data were single-channel models. Hood et al. suggested that adding separate M and P or ON and OFF channels may help. We will see that the presence of ON and OFF channels in Wilson's model is fundamental to its ability to predict probed-sinewave data in Fig. 1.

Methods

Wilson's model—General description

The model contains a "retinal module" which produces outputs for both M- and P-ganglion cells. To generate predictions for behavioral data, these retinal outputs are passed through a lowpass filter to simulate postretinal (cortical) filtering (Lee et al., 1990). We will refer to a class of ganglion cells (e.g. ON M cells) followed by the cortical filter as a pathway (e.g. M_{ON} pathway). The model may have shortcomings as a model of the retina *per se* (see Discussion here, and Hood, 1998), but here we are concerned only with the model's ability to predict behavioral data. In particular, we assess whether detection by the M-pathways in the model can predict data from the probed-sinewave paradigm.

Fig. 3 is a schematic of the model presented in a form to make it easier to compare to earlier models reviewed by Graham and Hood (1992b) and Hood et al. (1997). The main components of the M_{ON} -pathway are shown with some details omitted. In particular, the filtering due to the optics, a nonlinearity due to pigment bleaching, and spatial pooling of various signals are not included. The squares are lowpass filters which have one stage unless noted (e.g. $n = 3$ signifies three stages) and have a time constant of 5 ms unless noted. The dashed boxes surround three stages of nonlinear mechanisms. Stage one, identified by Wilson as the cone's output (C) after horizontal cell feedback (H), is a feedback subtractive process. The gain g of the feedback H, as well of its time course (τ_H/g), is controlled by a second feedback signal (P) that comes from stage 2. The time constant τ_P of this feedback signal (P) is long, 3 s, and thus for our purposes the value of g is essentially set by the time average luminance of the input. This element in the

model is conceptually similar, although not mathematically identical, to the feedback module in the Sperling and Sondhi (1968) model.

The second nonlinear stage (2) of the model is a multiplicative (called divisive by Wilson) feedback stage in which the input is divided by a feedback signal. The input to stage 2 is the difference between the signal C and the signal H. The feedback signal, identified as an amacrine cell output A, is formed by passing the output of this stage, B_{ON} , through a lowpass filter with a time constant τ_A of 80 ms. This multiplicative feedback stage is similar in some ways to the multiplicative (usually feedforward) stages used in the so-called MUSNL models reviewed by Graham and Hood (1992b). Together with stage 1, it produces the "frequency dependent gain control mechanisms" that Graham and Hood (1992b) identified as one of the four key components of computational models capable of predicting data from both periodic and aperiodic psychophysical paradigms. The same signal A that controls the multiplicative changes in this stage drives the signal P that affects the gain and time constant of the horizontal feedback (H) of stage 1.

The output of stage 3 in Fig. 3 is identified by Wilson as the response of the ON-center M-ganglion cell (M_{ON} ganglion cell). The input to stage 3 is the difference between B_{ON} and B_{OFF} , where B_{ON} is the signal from the stage 2 shown in Fig. 3 and identified as the ON-center M-bipolar and B_{OFF} is the nearly equal (factor of 0.9) inhibitory input from the stage 2 identified as the OFF-center M-bipolar cell. This push-pull input is truncated at zero and passed through a compressive, static nonlinearity (SNL). Together these two nonlinear operations are identified as SNL2 in Fig. 2. The push-pull mechanism has been employed in models of ganglion cell function (e.g. Gaudiano, 1994). There are also similarities here to the earlier MUSNL models reviewed by Graham and Hood (1992b). First, the compressive nonlinearity in SNL2 is identical in form to the SNL in these models. Further, the SNL in the earlier models was preceded by a subtractive stage that removed nearly all the steady-state response to a background. Since the steady-state responses of the B_{ON} and B_{OFF} are nearly equal, the push-pull mechanism removes about 90% of the steady-state response as originally suggested by Geisler (1981).

After a final four-stage lowpass filter, identified as being cortical by Wilson, the output of the M_{ON} pathway is produced.

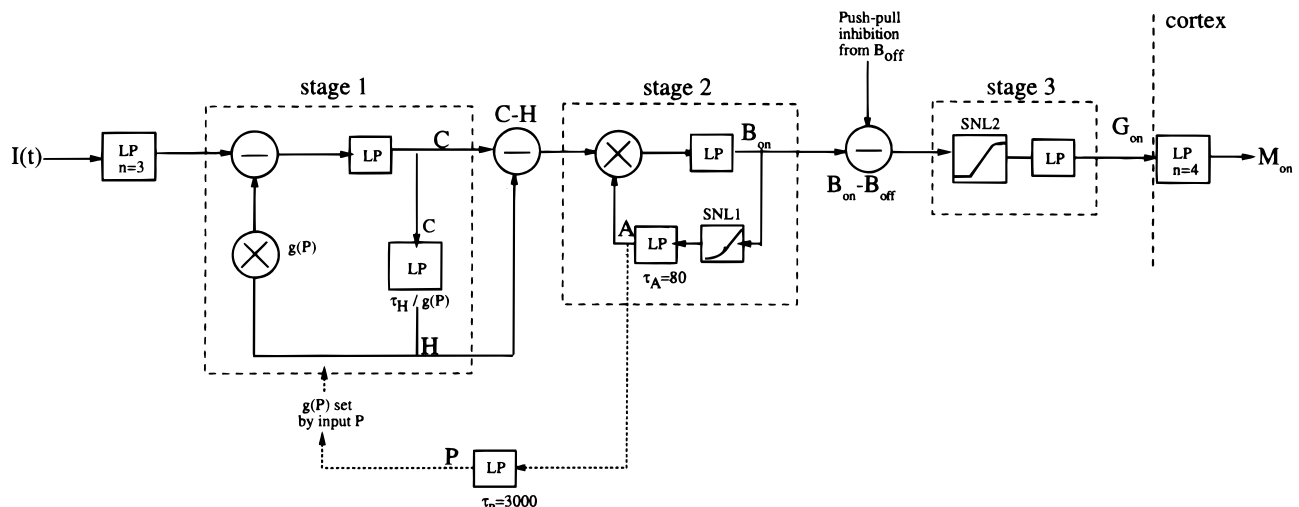


Fig. 3. A schematic of the M_{ON} -pathway in Wilson's model. See text and Wilson (1997) for details.

The model-specific parameters

By design, Wilson limited the scope of the model to achromatic stimuli presented to the central 1 deg of the fovea. Although the model accepts one-dimensional spatial patterns such as grating or bars, the simulations here assume that the stimuli cover the central 1 deg of the retina and only the temporal computability of the model is used. The version of the model used here is the same as that described by Wilson (1997). That is, all the parameters were set as described in that paper including the lowpass filter to simulate subsequent cortical filtering following the M-ganglion cell output. All simulations were done as if the probe and background field filled the whole field. For the relatively large stimuli used here, it is commonly assumed that the M-pathways are more sensitive than the P-pathways [see reviews by Lennie (1993) and Merigan & Maunsell (1993)]. We too make this assumption and show only the predictions for the ON and OFF M-pathways. However, our preliminary results suggest that the ΔI curves predicted for only the P-pathways of the model would have similar properties to those of the M-pathway.

The decision rule

A constant-response (peak-to-trough detection) rule was employed for the threshold decision. (See discussion of decision rules in Graham & Hood, 1992a.) In particular, the incremental response to the probe, ΔR , is defined as the response to the background plus probe minus the response to the background alone. The amplitude of ΔR is measured from the peak of the response to the trough of the response. And, the threshold ΔI is the value of the probe intensity for which ΔR equals a constant criterion response δ . The criterion value for ΔR was set equal to 1.0 (Wilson, 1997).

Predictions

Predicted thresholds for the probed-sinewave paradigm were generated using MATLAB by Math Works. [Code for the model was supplied by Hugh Wilson and modified to be compatible with programs previously employed to simulate the probed-sinewave experiment (Hood et al., 1997).] For Fig. 4, the simulations of the Hood et al. 1-Hz condition (Fig. 2B), the mean luminance was set to 250 td, the sinewave modulation had a contrast of 57%, and the probe's duration was 10 ms. For Fig. 5, the simulations of the Boynton et al. conditions (Fig. 1), the mean luminance was set to 250 td, the squarewave modulation had a contrast of 100%, and the probe's duration was 3 ms.

Results

The model's predictions

Fig. 4 shows the model's predictions for the 1-Hz condition (Fig. 2B) employed by Hood et al. (1997). The lowest trace in Fig. 4A is the background stimulus, a 1-Hz sinewave modulation. The solid curve immediately above it is the response of the M_{ON} -pathway to this stimulus. During the positive phase of the stimulus, this M_{ON} response is a distorted version of the stimulus waveform. And, during the negative portion of the stimulus it is maximally inhibited; due to the push-pull input the response is "clamped" at zero. Note also that the response leads the stimulus. That is, the peak of the response is occurring near 0 deg while the stimulus peaks at 90 deg. The response of the M_{OFF} -pathway (lower dashed

curve) is approximately a mirror image of the response of the M_{ON} -pathway shifted by 180 deg. The data points above both responses show the threshold value ΔI of the probe needed to meet the detection criterion (see Methods). When the M_{ON} - or M_{OFF} -pathway is inhibited, the values of ΔI for that pathway are very high and when the pathway is responding, the values of ΔI are relatively low. (Panels B and C will be described below.)

Similarly, Fig. 5A shows the model's predictions for the 30-Hz condition employed by Boynton et al. (1961). The lowest trace is the 30-Hz squarewave modulation of the background. The solid curve immediately above it is the response of the M_{ON} -pathway to this stimulus. The response is nearly sinusoidal with a phase lag of about 50 deg. We will see below that the phase is actually lagged by 410 deg, more than one cycle. The response of the M_{OFF} -pathway (lower of the dashed curves) is of the same shape but 180 deg out of phase compared to the response of the M_{ON} -pathway. The data points above these responses are the probe threshold values ΔI as described for Fig. 4. These ΔI curves are roughly sinusoidal in shape, but more peaked and 180 deg out-of-phase relative to the responses of the pathways. As with 1 Hz, when the M_{ON} - and M_{OFF} -pathways are inhibited, the values of ΔI are relatively high and when these pathways are responding, the values of ΔI are relatively low.

A comparison to the psychophysical data

To compare the model's predictions to the probed-sinewave data, we assume that the most sensitive pathway controls detection. Panels B in Figs. 4 and 5 show the ΔI curves from panel A expressed relative to the threshold on a steady background equal in luminance to the mean of the modulated background. The symbols are enlarged when they represent ΔI values for the most sensitive pathway and hence the observer. (Where the values were very close both are shown enlarged.) The resulting ΔI curves (shown as bold) for the observer are partially mediated by M_{ON} - and partially mediated by M_{OFF} -pathways.

The predictions for the 1-Hz condition (Fig. 4B) bear some resemblance to the behavioral data in Fig. 2B. However, the predictions for the 30-Hz condition (Fig. 5B) do not resemble the behavioral data in Fig. 1. The Boynton et al. data in Fig. 1 peak at about 90 deg while the predictions in Fig. 5B peak at 180 deg, and, the data approximate a sinusoid while the predictions show two peaks per cycle.

A simple assumption, however, brings the predictions for both conditions much closer to the data. If we assume that the M_{ON} -pathway is two times less sensitive than the M_{OFF} , then the predictions shown in panel C of Figs. 4 and 5 result. (As in panel B, the small symbols show the ΔI values for the M_{ON} - and M_{OFF} -pathways, and the large symbols connected by the bold lines show the ΔI values for the most sensitive pathway.) In this case, the M_{ON} values are multiplied by a factor of 2. Although this assumption was added *post hoc*, there is a justification in the literature which will be considered in the Discussion. This adjustment has a qualitatively different effect for the two conditions. For the 1-Hz condition, portions of the ΔI curve are still attributed to detection by the M_{ON} -pathway but thresholds are higher. In the case of 30 Hz, detection is essentially entirely mediated by the M_{OFF} -pathway. These new predictions bear some striking similarities to aspects of the probed-sinewave data. For the 1-Hz condition, the predicted curves capture the general shape as well as the phases of the peak and trough of the data in Fig. 2B. For the 30-Hz condition, both data (Fig. 1) and predictions are roughly sinusoidal in shape with

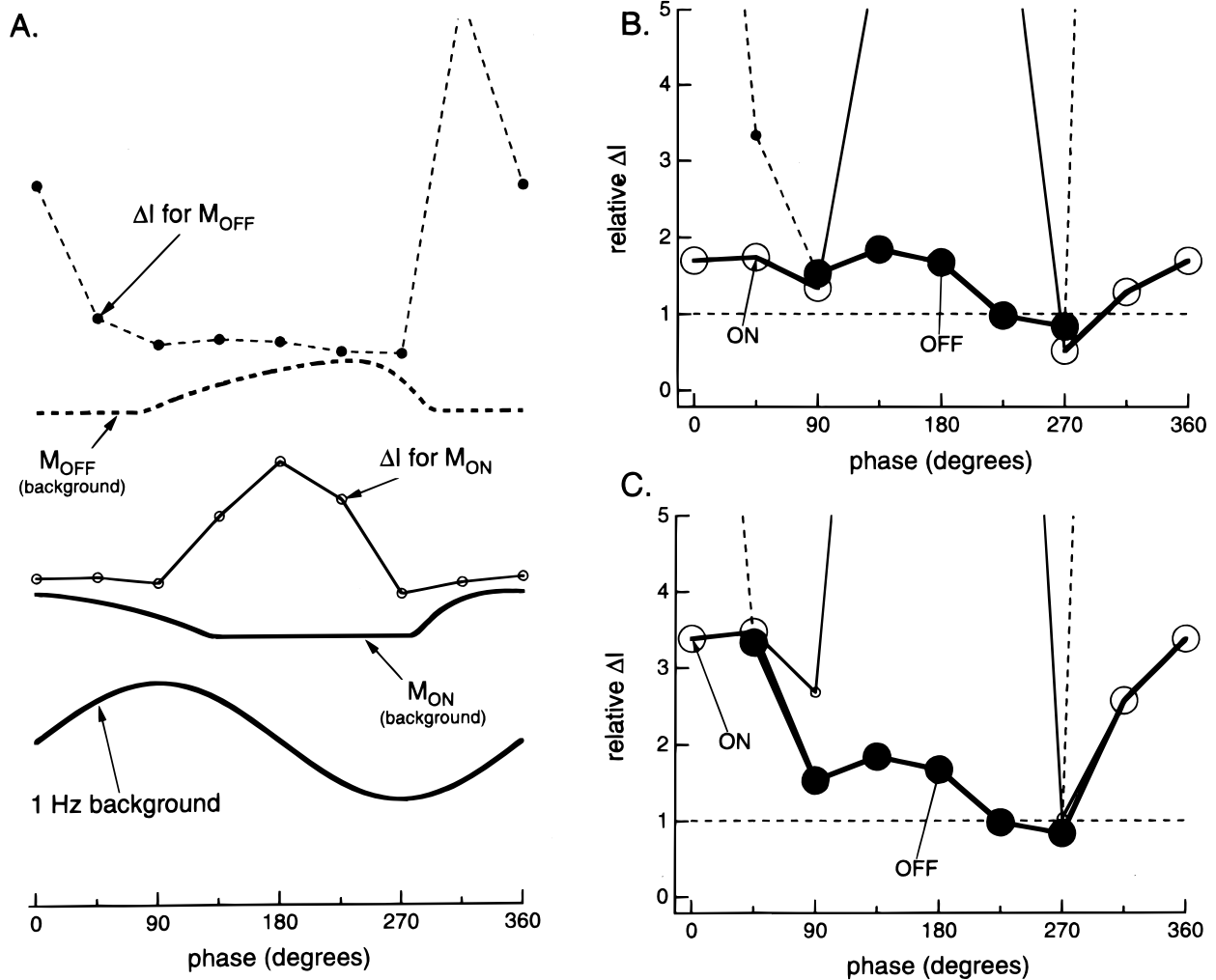


Fig. 4. Simulations of the Hood et al. (1997) 1-Hz condition (Fig. 2). A: The solid and dash curves labeled “ M_{ON} ” and “ M_{OFF} ” are the responses of the M_{ON} - and M_{OFF} -pathways to the 1-Hz background shown as the bold curve labeled “1 Hz background”. The data points show the ΔI curves for the M_{ON} -pathway (open symbols) and M_{OFF} -pathway (filled symbols). B: The ΔI curves for both pathways (open symbols: M_{ON} -pathway; filled symbols: M_{OFF} -pathway) are each plotted relative to the pathway’s threshold on a steady background (0 Hz) of the same mean luminance as the modulated background. The large symbols indicate the most sensitive pathway at each phase. Where the thresholds of the two pathways are close, they are both shown. C: The same as in panel B with the added assumption that the M_{ON} -pathway is two times less sensitive than the M_{OFF} -pathway.

a peak at 90 deg. Further, there is an unmodulated, or dc shift, apparent in the predictions as there is in the data of Boynton et al. (see their Fig. 5).

Simulations for a range of frequencies

For both the ON and OFF pathways, the predicted ΔI curves for the 1-Hz condition lead the stimulus and are distinctly nonsinusoidal while the ΔI curves for the 30-Hz condition nearly follow the stimulus in phase and shape. These two sets of predictions were run with different stimulus parameters in order to make comparisons to existing data (see Methods). To obtain a deeper understanding of the change with background frequency, simulations were run for a range of frequencies under the stimulus parameters employed for the 1-Hz condition (a mean luminance of 250 cd/m² and a contrast of 57%). [The reader uninterested in this level of detail can precede to the Discussion.]

The curves in Fig. 6A are the responses of the M_{ON} -pathway to the background alone for a range of frequencies from 1 to 42 Hz. The responses to the higher frequencies have been scaled as indicated on the graph. The stimulus (not shown) has a phase of 0 deg (stimulus peak at 90 deg). The phase of the peak of these M_{ON} -pathway responses is shown as a function of frequency as the solid curve in Figs. 8A and 8B. Notice that the response peak occurs at -10.8 deg for the 1-Hz background and at 575 deg for the 42-Hz background (also see the “Xs” in Fig. 6A). Thus, since the stimulus peaks at 90 deg, the phase of the peak response goes from leading the background stimulus by 100.8 deg at 1 Hz to lagging it by 485 deg at 42 Hz.

Fig. 7 shows the ΔI curves for the M_{ON} -pathway. (The scale for panel B is expanded by a factor of 10 and the results for 24 Hz are presented in both panels.) The maximum of the ΔI curves shifts from 180 deg to 270 deg and then back to 180 deg as the frequency of the background is increased (see arrows with numbers in Fig. 7).

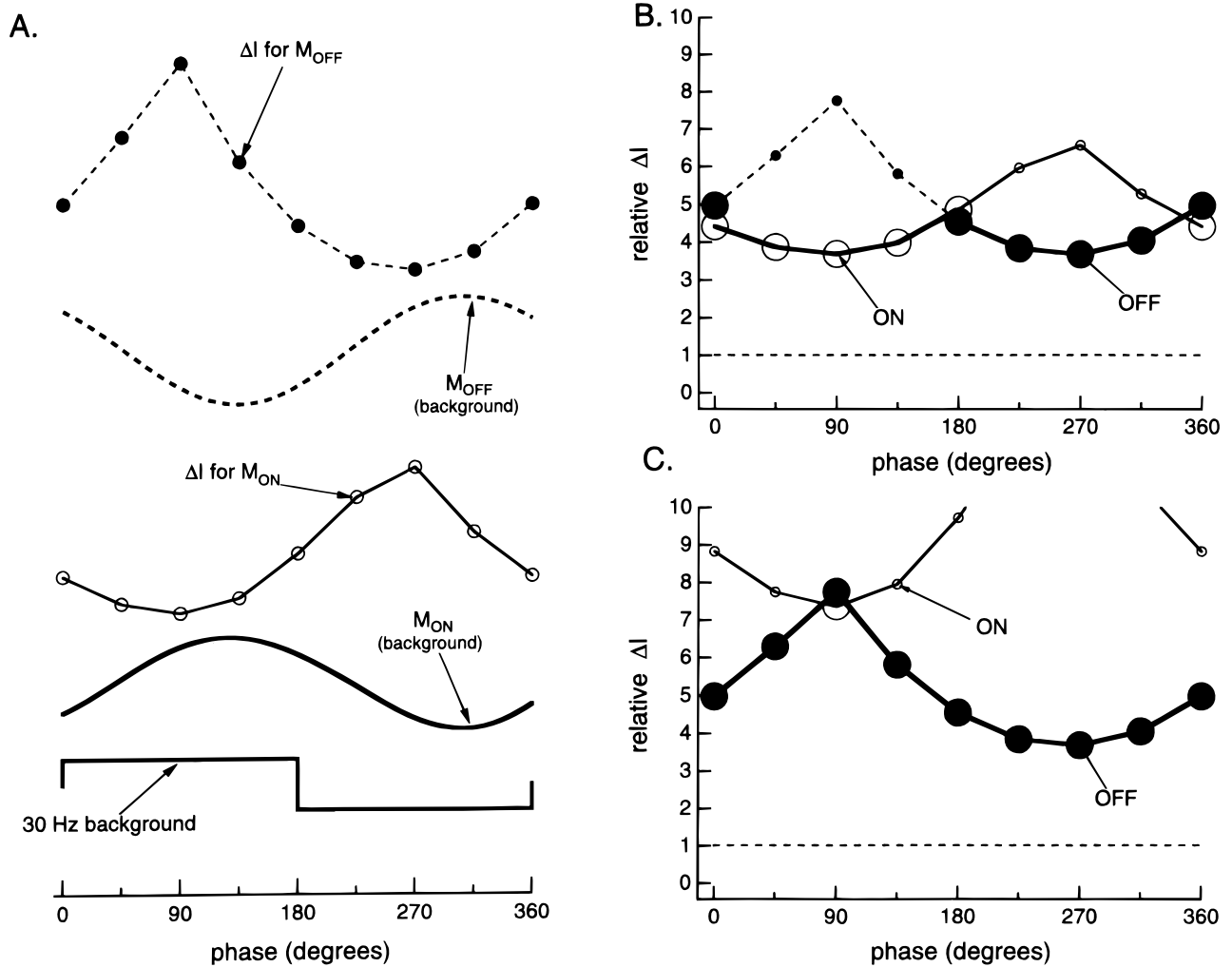


Fig. 5. Simulations of the Boynton et al. (1961) 30-Hz conditions (Fig. 1). A: The solid and dash curves labeled “ M_{ON} ” and “ M_{OFF} ” are the responses of the M_{ON} - and M_{OFF} -pathways to the 30-Hz squarewave background shown as the bold curve labeled “30 Hz background”. The data points show the ΔI curves for the M_{ON} -pathway (open symbols) and M_{OFF} -pathway (filled symbols). B: As in Fig. 4. C: As in Fig. 4.

Fig. 8B shows the phases of the maxima of these ΔI curves as the open symbols. The results of a similar analysis for the M_{OFF} -pathway are shown as the filled symbols in Fig. 8B.

To understand the relationship between the maxima of the ΔI curves and the excitatory and inhibitory phases of the responses to the background, the delay of the response to the probe must be taken into consideration. As an example, consider the probes presented at 0 deg for 1 Hz and 42 Hz. The incremental responses to these probes are shown in Fig. 6B (as solid curves) superimposed on the background responses to 1 and 42 Hz (as dashed curves, repeated from panel A). These probe responses were vertically scaled so as to be easily visible. Notice how brief the probe response appears on the 1-Hz background and how prolonged and delayed it appears on the 42-Hz background. The peak of the response to the probe is occurring with a lag of 15 deg on the 1-Hz background and a lag of 635 deg on the 42-Hz background. These two probe responses are shown plotted against time rather than phase in Fig. 6C. Notice now the responses have about the same shape and about the same time to peak. The peaks occur approximately at 42 ms following the probe onset. To a first approxima-

tion, the peak response to the probe has a constant latency of about 42 ms independent of the background frequency. [This constancy probably reflects the fact that the probe always has the same frequency composition.] The dotted curve in Fig. 8A shows the delay of the probe, assuming a 42-ms delay, in terms of phase of the background. As the frequency of the background is made higher, the response to the background is delayed in terms of phase (solid curve in Fig. 8A), but so is the phase at which the response to the probe occurs (dotted curve in Fig. 8A). These delays are not identical. (If the model acted like constant delay filter of 42 ms, then these would be the same.) The difference between these curves gives the phase shifts of the peak probe response relative to the peak background response and is shown as the dashed curve in Fig. 8A.

This curve of phase shifts supplies a good fit to the phase of the maximum of the ΔI curve for the M_{OFF} -pathway as shown by the dashed curve through the filled symbols in Fig. 8B. The success of this fit indicates that the maximum of the ΔI curves for the M_{OFF} -pathway occurs 180 deg out of phase with the peak of the excitatory phase of the M_{OFF} -pathway, presumably because it is occurring at the peak of the inhibitory phase. Shifting this curve by 180 deg

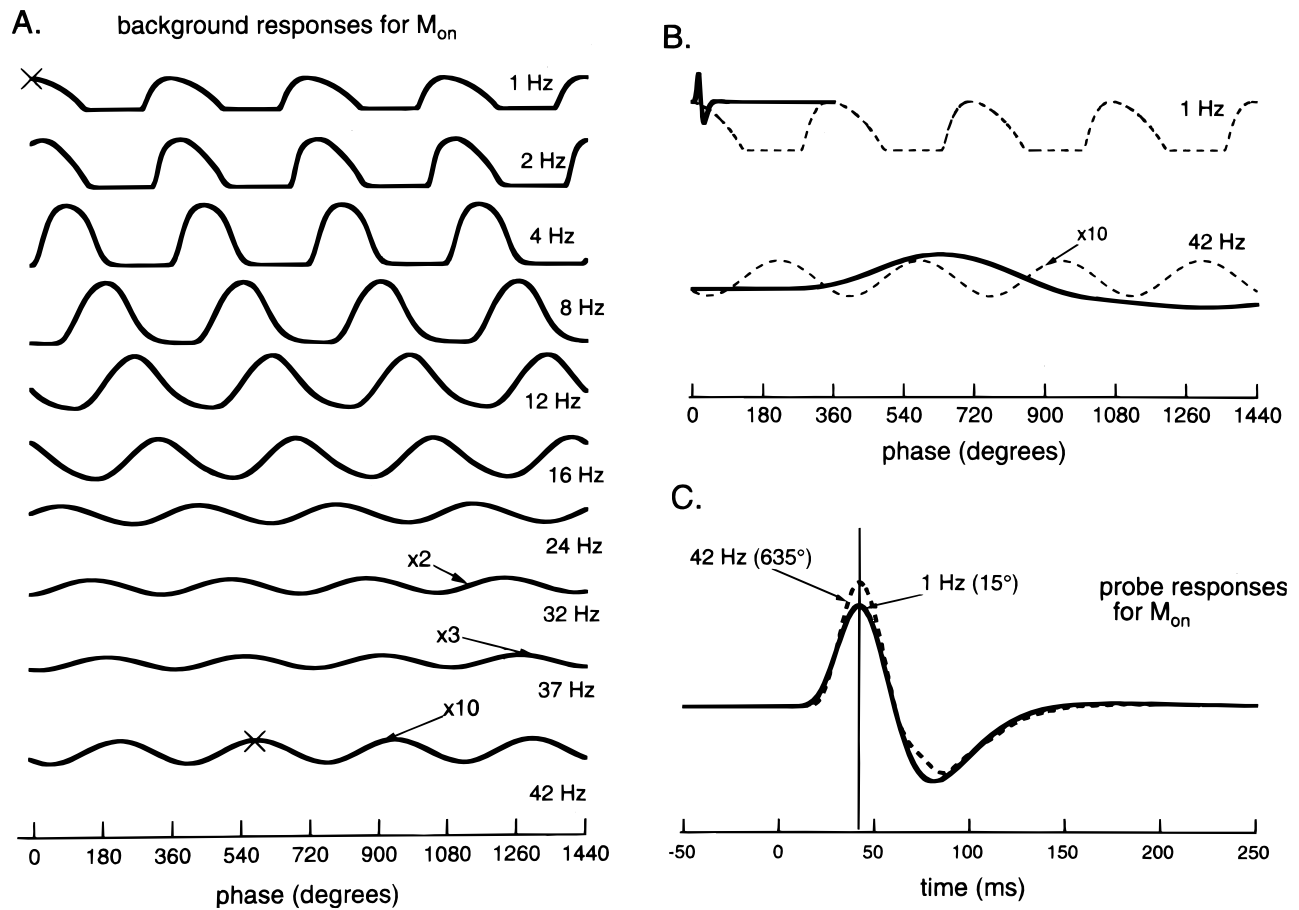


Fig. 6. A: The curves are the response of the M_{ON} -pathway to a range of background frequencies. As in Figs. 2 and 4, the mean luminance was 250 cd/m² and the contrast was 57%. The responses to the higher frequencies were scaled by the amounts shown so that they could be seen. B: The dashed curves are the responses to the 1- and 42-Hz backgrounds from panel A. The solid curves show the response to the probe (not to scale) presented at phase 0 deg. C: The probe responses shown in panel B (solid curves) are plotted on a time axis.

provides a reasonably good fit to the phases of the maximum of the ΔI curves for the M_{ON} -pathway as shown by the solid curve through the open symbols in Fig. 8B presumably for analogous reasons.

The success of these fits makes it easier to understand the ΔI curves in Fig. 7 in terms of excitation and inhibition. The peak of the ΔI curve for a single pathway, M_{ON} in Fig. 7, occurs when the peak of the probe response falls at the maximally inhibited portion of the response to the background. The excitatory portion of the response to the background leads to relatively low ΔI values. To understand what is happening to ΔI during the excitatory portion, consider the place in the ΔI curve that is 180 deg out of phase with the peak of the inhibition. These points are marked with the asterisk in Fig. 7. For high frequencies, above 24 Hz, the asterisk marks a local minimum, and the ΔI curve has only a single peak. For low frequencies, below 12 Hz, the asterisk marks a local maximum, and the ΔI curve has two peaks.

To obtain a better understanding of the mechanisms contributing to these frequency-dependent differences, the model was modified and simulations run for a low and high background frequency. To examine the role of the push-pull mechanism, the push-pull inhibitory input to the pathways was removed (the inhibition from B_{OFF} in Fig. 3). Simulations were run for backgrounds of 1 and 32 Hz under the same conditions as Figs. 4 and 7 (a mean lumi-

nance of 250 cd/m² and a contrast of 57%). All ΔI values were expressed relative to the threshold of the probe on a steady field of the same mean luminance. Fig. 9 shows the ΔI for the M_{ON} -pathway without push-pull inhibition (filled circles) along with the ΔI values for this pathway with push-pull inhibition (open circles, from Fig. 7). Removing the push-pull mechanism eliminates the peak in the ΔI curve associated with the inhibitory portion of the response. This peak elevation in threshold is attributable to the inhibitory input coupled with the nonlinearity (SNL2 in Fig. 3) that does not let the input to the ganglion cell go below zero. Without the inhibitory input, the phase that was once associated with the peak of the ΔI curve is now near, in the case of 1 Hz, or at, in the case of 32 Hz, the lowest ΔI value. Removing the push-pull mechanism also eliminates the large dc shift present in the ΔI curve for 32 Hz. The push-pull mechanism is not, however, the only factor contributing to this shift. The cortical filter plays a role. To examine this role, the stimulations were repeated for the model's output G_{ON} before the final filtering. The results are shown as the \times symbols in Fig. 9. There is little difference for the 1-Hz condition, but the dc level is lower for the 30-Hz condition.

These simulations suggest that the shape of the ΔI curve for higher frequencies in Fig. 7 is being largely determined by the inhibitory push-pull mechanism, and thus there is a local mini-

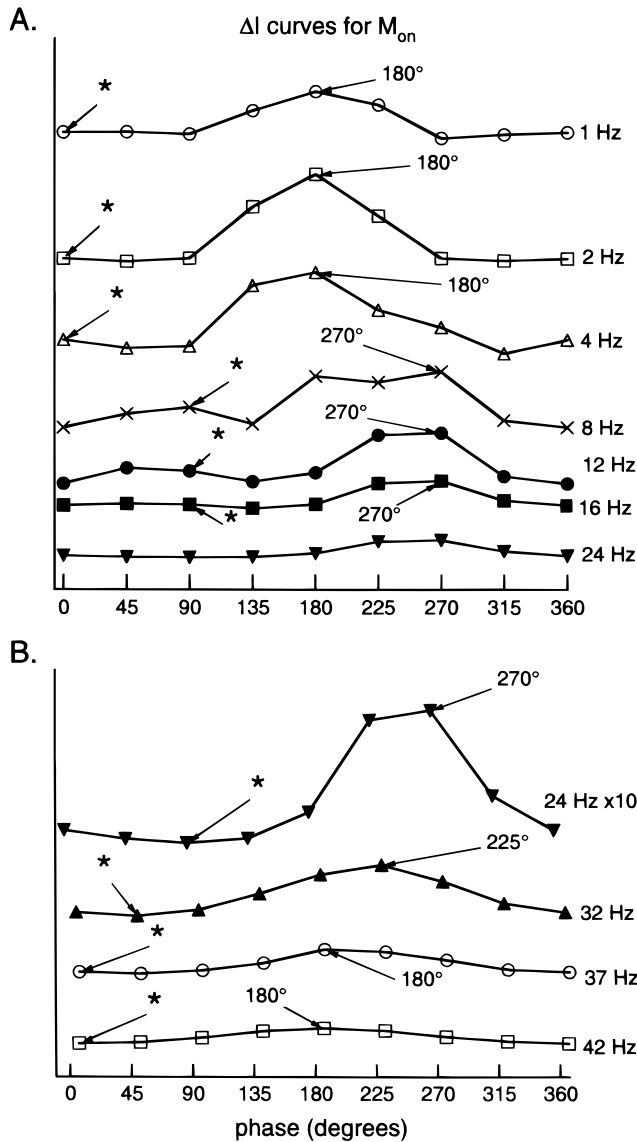


Fig. 7. A: ΔI curves for the M_{ON} -pathway. The maximum threshold is indicated by the arrow and the point 180 deg away from the maximum by the asterisk. B: As in panel B but the ΔI scale is 10 times that in panel A.

imum in the ΔI curve that appears 180 deg out-of-phase with the local maximum caused by the peak of the inhibition. The push-pull mechanism is very important at the lower background frequencies as well, since it produces the largest peak in the ΔI curve for a single pathway, but other mechanisms (e.g. the multiplicative adaptation stage 3 and the static nonlinearity, SNL2, in Fig. 3) also contribute by decreasing the response to the probe during the excitatory phase of the background response, thereby elevating ΔI and producing a second peak in the ΔI curve for a single pathway.

Discussion

The simulations with Wilson’s model successfully predict some of the fundamental aspects of the probed-sinewave data. For the 1-Hz condition, the fact that the maximum and minimum of the ΔI

curves are 270 deg apart can be attributed to the contributions of ON and OFF pathways to detection at different phases (see Fig. 4C). According to the analysis here, for the 1-Hz background, detection is mediated by the ON pathway at the maximum of the ΔI curve (at about 0 deg) and by the OFF pathway at the lower values of the ΔI curve (between about 90 and 270 deg).

The story differs for high frequencies, including the 30-Hz data of Boynton et al. (1961). Here the OFF pathway is mediating detection at all phases (see Fig. 5C). The ΔI curve is at a maximum at the trough of the background response of this pathway (during peak inhibition) and at a minimum at the peak of the background response (during peak excitation). Further, ΔI is approximately 180 deg out-of-phase with the response of the OFF pathway to the background, but approximately in phase with the stimulus. The actual relationship between the stimulus and the ΔI curves will depend upon the relative phases of the responses to the probe and the background. We should expect that, in general, the data for high temporal frequencies would appear approximately sinusoidal but that the data need not be exactly in phase with the stimulus (see Fig. 8B). Recent measurements for high temporal frequencies show that although the peak of the ΔI curve is in phase for a 30-Hz background, it is out-of-phase for a 20-Hz background (Wu et al., 1997).

Fig. 10 illustrates our explanation for the Boynton et al.’s results. The upper part of Fig. 10 shows the 30-Hz squarewave background stimulus (dashed curve) and the response (solid curve) of the M_{OFF} -pathway to this background. According to the model’s simulations, this response to the background is delayed by 395 deg—as indicated by the arrow marked “phase shift (background)” —and is approximately sinusoidal because of the lowpass filtering of the model. The response is also inverted relative to the stimulus because it is the response of an OFF pathway. The lower two curves show the incremental response to a probe of constant intensity presented at 90 deg (dotted) or 270 deg (solid). The peak-to-trough response to the probe is considerably smaller at 90 deg than at 270 deg; therefore, ΔI is larger at 90 deg than at 270 deg. Since the responses to the probe and background are shifted by about the same amount at 30 Hz, the response to a probe presented at 90 deg falls during the peak of the push-pull inhibition resulting in a maximum ΔI . [The phase shift for the probe—indicated by the arrow labeled “phase shift (probe)” —is actually slightly longer, around 416 deg, than is the phase shift (395 deg) of the background.] And the response to a probe presented at 270 deg falls during the period about 180 deg from the peak inhibition resulting in a minimum ΔI . Thus for the 30-Hz condition, ΔI is approximately in phase with the stimulus because it is 180 deg out of phase with the response to the background which in turn is approximately 180 deg out of phase with the stimulus.

Finally, the model successfully predicts the unmodulated, or dc component, of the probe-sinewave data at 30 Hz. In particular, the mean probe threshold is elevated above its value on a steady background and this elevation is greater for the higher frequency (see Figs. 4C and 5C). We initially thought that the fast multiplicative stage (stage 2 in Fig. 3) might contribute to this dc shift since its time constant, 80 ms, is short relative to the 1-Hz stimulus but long relative to higher background rates. Our simulations (not shown) suggest that while this stage may contribute some to the differences in dc level, it is a relatively minor factor. The push-pull input to the ganglion cell appears to be the main factor contributing to the dc or unmodulated threshold elevation although the final filter in the model plays a role at high modulation rates (see Fig. 9).

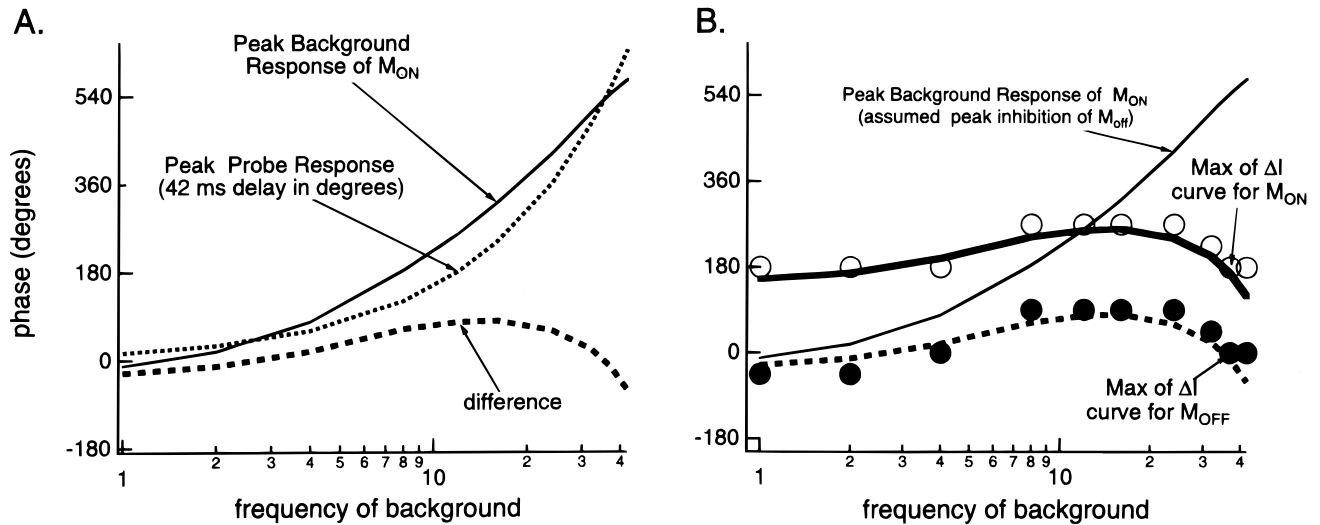


Fig. 8. A: The phase at which the maximum response to the background (solid curve) and probe (dotted curve) occurs is shown as a function of the background frequency. The phase of the background’s response was measured from the curves in Fig. 6A. The phase of the probe’s response was calculated by assuming that its peak occurred at 42 ms following its presentation. This assumption was confirmed by measuring the time to peak of probe responses over a range of conditions. The bold dashed curve is the difference between the solid and dotted curves. B: The phase at which the maximum of the ΔI curve occurs is shown as a function of the background frequency for the M_{ON}-pathway (open symbols-see also arrows in Fig. 7) and M_{OFF}-pathway (filled symbols). The bold dashed curve is the curve marked “difference” in panel A and the bold solid curve is this curve shifted vertically by 180 deg.

ON versus OFF pathway sensitivity

To produce plausible predictions from the model, we had to assume that the ON pathway was less sensitive than the OFF pathway by a factor of two. This factor was not determined based upon a best fit but it is clear that it cannot be much less than 2 (in fact, not less than about 1.7) and still provide a good description of the 30-Hz data nor can it be much more than two and provide a good description of the 1-Hz data. Although the assumed difference in

sensitivity was purely *post hoc*, it is supported by two lines of evidence. First, other psychophysical data have been offered in support for separate ON and OFF pathways with different sensitivities. A number of studies have found that thresholds for decrements were lower than for increments by about 1.5 (e.g. Boynton et al., 1964; Krauskopf, 1980). Further, thresholds for sawtooth stimuli that have an abrupt onset (a rapid-on shown to favor M_{ON}) can be as much as 1.5 higher than thresholds for sawtooth stimuli with an abrupt offset (a rapid-off shown to favor M_{OFF}), although

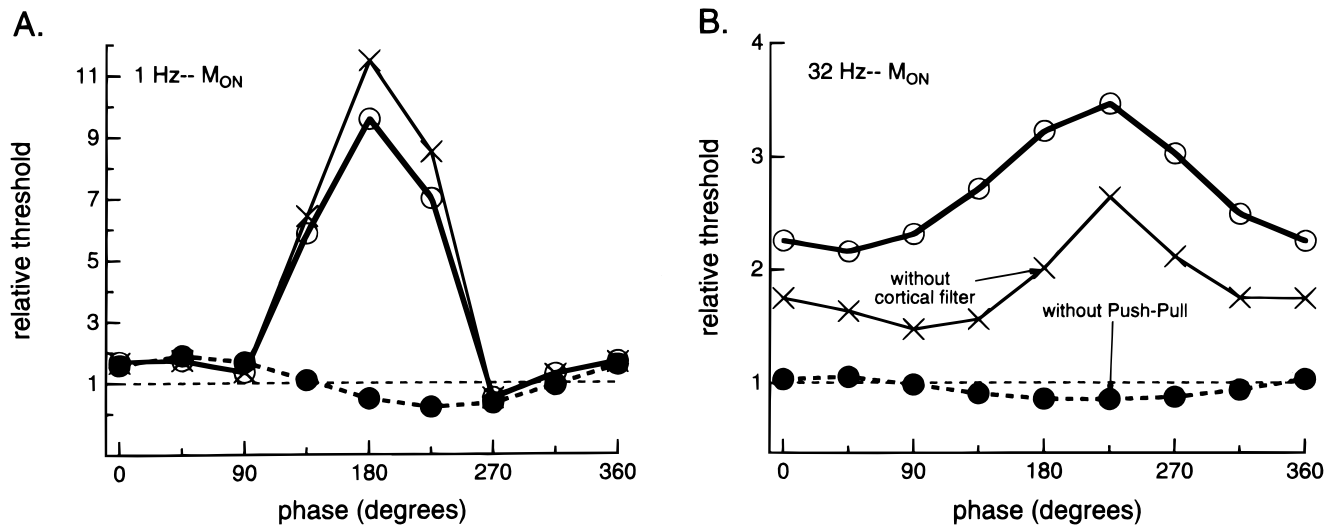


Fig. 9. A: The open symbols are the ΔI curve for the M_{ON}-pathway from Fig. 7A for the 1-Hz background condition. The other two curves are the ΔI curves derived from the model by removing the cortical filter (× symbols) or the push-pull mechanism (filled symbols). B: Same as in panel A for the 32-Hz background condition.

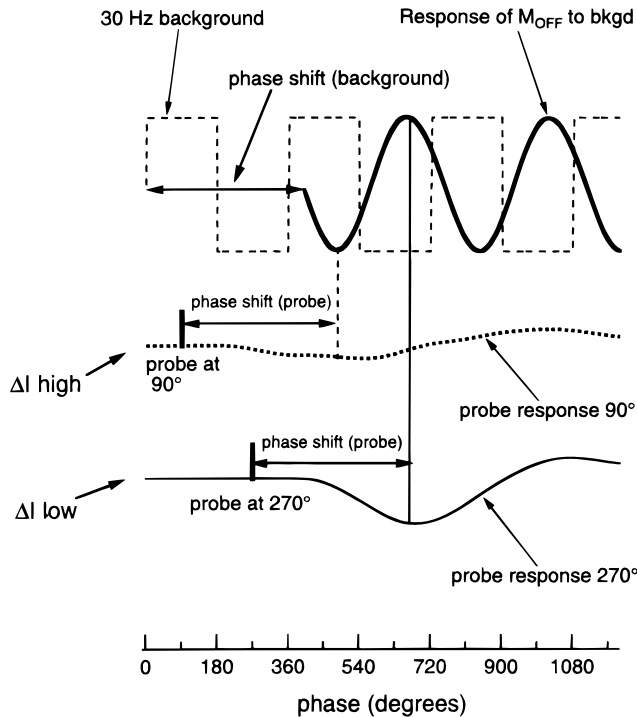


Fig. 10. A schematic illustrating the factors involved in the Boynton et al. (1961) finding that increment threshold (ΔI) appears to be following the modulation of a 30-Hz background (see Fig. 1). See text for details.

the difference between rapid-on and -off thresholds diminishes at higher temporal frequencies (Bowen et al., 1989, 1992; Kremers et al., 1993). A second line of evidence for a greater sensitivity of the OFF pathways was provided in a study of human visual evoked potentials (VEP). Zemon et al. (1988) recorded VEPs to increments or decrements in contrast, and argued based upon these recordings that the cortical OFF pathways were two times more sensitive than the cortical ON pathways. Thus, at this point we can cautiously conclude only that our assumed difference in ON and OFF pathway sensitivities is plausible and that it will need further testing.

Implications for computational models

There are general implications here for computational models that seek to predict the probed-sinewave data. For example, considerably less than Wilson's full model is needed to predict the 30-Hz results. The following conditions would be sufficient: (1) a single pathway mediates detection; (2) this pathway follows a 30-Hz squarewave or sinewave modulation with a phase lag that is approximately equal to the phase lag of the probe's response; and (3) this pathway has a mechanism to elevate ΔI during the inhibitory phase of the response to the background if the pathway is an OFF pathway or during the excitatory phase of the response if the pathway is an ON pathway. It is more difficult to describe the sufficient conditions a model must meet in order to predict the 1-Hz data. But, a key aspect of Wilson's model is the presence of two detecting mechanisms (e.g. ON and OFF pathways).

Concluding remarks

Wilson's model is one of the first to explicitly predict both the retinal output (ganglion cell responses) and a range of behavioral

data. Some of the strengths and weakness of existing computational models of light adaptation, including this model, have been reviewed recently (Makous, 1997; Hood, 1998). It is worth repeating here that there are primate ganglion cell data that the retinal component of Wilson's model should predict but does not. Our simulations indicate, for example, that the predictions do not show retinal contrast gain control as defined by Shapley and Victor (1979). In particular, the function relating ganglion cell response to the temporal frequency of the stimulus does not change with stimulus contrast level for the predictions as it does for primate ganglion cells (e.g. Benardete et al., 1992). Further, too little is known about primate retinal physiology to believe that the details of the retinal circuitry in the model will be correct. In addition, there is at least one mechanism included in the retinal component of Wilson's model that is probably cortical. In particular, the bulk of the evidence argues for the push-pull mechanism being postretinal (see review by Hood, 1998). This is interesting as our simulations indicate that the push-pull mechanism is particularly important in producing the results reported here. Without this mechanism, there would be little dc elevation, the shape of the responses to 1 Hz would be sinusoidal and the ΔI curves for 30 Hz would be shifted by 180 deg (see Fig. 9). However, although aspects of Wilson's model may need modifying for other purposes such as predicting retinal output, this is not critical here. For now, we make no assumptions about where the mechanisms are located, but conclude only that Wilson's model successfully predicts a range of psychophysical data including previously unexplained aspects of probed-sinewave data.

Although here we explicitly compared the model's predictions to the 1-Hz data from Hood et al. (1997) and the high-frequency data from Boynton et al. (1961), there is general qualitative agreement with the low- and high-frequency data from other published studies (Shickman, 1970; Maruyama & Takahashi 1977; Wu et al., 1997). We avoided predicting the data for intermediate (e.g. around 10 Hz) because there is poor agreement among existing studies (cf. Shickman, 1970; Maruyama & Takahashi, 1977; Hood et al., 1997). However, some of these data (e.g. Hood et al., 1997) do not conform to the model's predictions derived here. But, these are the conditions where our simulations (see Fig. 4B) suggest the shape of the ΔI curves could be most volatile due to a change from mixed ON and OFF pathways to OFF pathways as well as the relative location of the peaks in the ΔI and background responses. It remains to be seen whether adjustments in the model will allow it to predict the results from different laboratories. The challenge for the near future will be to predict probed-sinewave data from the same subjects with a range of background luminance, contrast, and frequency conditions.

Acknowledgments

This research was supported by National Eye Institute Grants EY-02115 and EY-08459 to D. Hood and N. Graham, respectively. We thank Hugh Wilson for supplying the MATLAB code for his model and for his helpful advice and Sabina Wolfson for her helpful comments on the manuscript. A preliminary version of some of this material was presented at the 1997 annual meeting of the Optical Society of America.

References

- BENARDETE, E.A., KAPLAN, E. & KNIGHT, B.W. (1992). Contrast gain control in the primate retina: P-cells are not X-like, some M-cells are. *Visual Neuroscience* **8**, 483–486.
- BONE, R.A. & CHEN, Y.P. (1995). Improved temporal gain and phase

- measurements (5–45 Hz) leading to a triphasic impulse response. *Investigative Ophthalmology and Visual Science* (Suppl.–Abstract) **36**, S906.
- BOWEN, R.W., POKORNY, J. & SMITH, V.C. (1989). Sawtooth contrast sensitivity: Decrements have the edge. *Vision Research* **29**, 1501–1509.
- BOWEN, R.W., POKORNY, J., SMITH, V.C. & FOWLER, M.A. (1992). Sawtooth contrast sensitivity: Effects of mean illuminance and low temporal frequencies. *Vision Research* **32**, 1239–1247.
- BOYNTON, R., STURR, J. & IKEDA, M. (1961). Study of flicker by increment threshold technique. *Journal of the Optical Society of America* **51**, 196–201.
- BOYNTON, R.M., IKEDA, M. & STILES, W.S. (1964). Interactions among chromatic mechanisms as inferred from positive and negative increment thresholds. *Vision Research* **4**, 87–117.
- CHASE, V.M., WIEGAND, T.E., HOOD, D.C. & GRAHAM, N. (1993). Exploring the dynamics of light adaptation using a sinusoidally modulated background and a probe. *Investigative Ophthalmology and Visual Science* (Suppl.–Abstract) **34**, 1036.
- GAUDIANO, P. (1994). Simulations of X and Y retinal ganglion cell behavior with a nonlinear push–pull model of spatiotemporal retinal processing. *Vision Research* **34**, 1767–1784.
- GEISLER, W.S. (1981). Effects of bleaching and backgrounds in the flash response of the cone system. *Journal of Physiology* **312**, 413–434.
- GRAHAM, N. & HOOD, D.C. (1992a). Quantal noise and decision rules in dynamic models of light adaptation. *Vision Research* **32**, 779–787.
- GRAHAM, N. & HOOD, D.C. (1992b). Modeling the dynamics of light adaptation: The merging of two traditions. *Vision Research* **32**, 1373–1393.
- HOOD, D.C. (1998). Lower-level visual processing and models of light adaptation. *Annual Review of Psychology* **49**, 503–535.
- HOOD, D.C. & FINKELSTEIN, M.A. (1986). Sensitivity to light. In *Handbook of Perception and Human Performance, Vol. 1: Sensory Processes and Perception*, ed. BOFF, K.R., KAUFMAN, L. & THOMAS, J.P., New York: John Wiley & Sons. 5-1–5-66.
- HOOD, D.C., GRAHAM, N., VON WIEGAND, T. & CHASE, V.M. (1997). Probed-sinewave paradigm: A test of models of light-adaptation dynamics. *Vision Research* **37**, 1177–1191.
- KRAUSKOPF, J. (1980). Discrimination and detection of changes in luminance. *Vision Research* **20**, 671–677.
- KREMERS, J., LEE, B.B., POKORNY, J. & SMITH, V.C. (1993). Responses of macaque ganglion cells and human observers to compound periodic waveforms. *Vision Research* **33**, 1997–2011.
- LEE, B.B., POKORNY, J., SMITH, V.C., MARTIN, P.R. & VALBERG, A. (1990). Luminance and chromatic modulation sensitivity of macaque ganglion cells and human observers. *Journal of the Optical Society of America* **7**, 2223–2236.
- LENNIE, P. (1993). Roles of M and P pathways. In *Contrast Sensitivity*, ed. SHAPLEY, R. & LAM, D.M.K., pp. 201–213. Cambridge Massachusetts: MIT Press.
- MAKOUS, W.L. (1997). Fourier models and the loci of adaptation. *Journal of the Optical Society of America A* **14**, 2323–2345.
- MARUYAMA, K. & TAKAHASHI, M. (1977). Wave form of flickering stimulus and visual masking function. *Tohoku Psychologica Folia* **36**, 120–133.
- MERIGAN, W.H. & MAUNSELL, J.H.R. (1993). How parallel are the primate visual pathways? *Annual Review of Neuroscience* **16**, 369–402.
- POWERS, M.K. & ROBSON, J.G., (1987). Sensitivity changes induced by temporal modulation of a background. *Investigative Ophthalmology and Visual Science* (Suppl.–Abstract) **28**, 357.
- SHAPLEY, R.M. & ENROTH-CUGELL, C. (1984). Visual adaptation and retinal gain controls. In *Progress in Retinal Research, Vol. 3*, ed. OSBORNE, N.N. & CHADER, G.J. pp. 263–343. Oxford: Pergamon Press.
- SHAPLEY, R.M. & VICTOR, J.D. (1979). The contrast gain control of the cat retina. *Vision Research* **19**, 431–434.
- SHICKMAN, G.M. (1970). Visual masking by low-frequency sinusoidally modulated light. *Journal of the Optical Society of America* **60**, 107–117.
- SPERLING, G. & SONDHI, M.M. (1968). Model for visual luminance discrimination and flicker detection. *Journal of the Optical Society of America* **58**, 1133–1145.
- SUN, V.C.W., POKORNY, J. & SMITH, V.C. (1995). Increment thresholds on temporally modulated backgrounds. *Journal of the Optical Society of America* (meeting) **88**.
- VON WIEGAND, T.E., HOOD, D.C. & GRAHAM, N.V. (1995). Testing a computation model of light-adaptation dynamics. *Vision Research* **35**, 3037–3051.
- WILSON, H.R. (1997). A neural model of foveal light adaptation and afterimage formation. *Visual Neuroscience* **14**, 403–423.
- WU, S., BURNS, S.A., ELSNER, A.E., ESKEW, R.T. & HE, J. (1997). Rapid sensitivity changes on flickering backgrounds: Tests of models of light adaptation. *Journal of the Optical Society of America* **14**, 2367–2378.
- ZEMON, V., GORDON, J. & WELCH, J. (1988). Asymmetries in On and Off visual pathways of humans revealed using contrast-evoked cortical potentials. *Visual Neuroscience* **1**, 145–150.